Anti-counterfeiting Measure Based on Magnetic Flux Density for Lithium-ion Batteries

Masahito Tsukano [*1] ***Naoki Noguchi*** [*1] ***Minako Terao*** [*1]
Miwa Tobita [*1] ***Kazuma Takenaka*** [*1] ***Jun Okano*** [*2]
Yukiko Onoue [*3] ***Kaoru Omichi*** [*2] ***Yuki Tominaga*** [*2]

This research proposes principles of an anti-counterfeiting measure based on magnetic flux density for lithium-ion batteries. Manufacturing of lithium-ion batteries is expected to increase with the growing use of electric vehicles as a countermeasure to global warming. However, those batteries are likely to be targets for theft or replacement with counterfeits because they contain rare materials. In this research, we verified that batteries generate magnetic flux density that is unique to the manufacturer or to even individual batteries since errors in assembly cause changes in this parameter. Throughout the experiment, we found that prismatic cells generate magnetic flux density corresponding to the product type whereas individually unique magnetic flux density was observed for battery packs with cylindrical cells. These principles are applicable as an anticounterfeiting measure since the uniqueness is hard to reproduce in counterfeits.

INTRODUCTION

Global warming is rapidly accelerating due to increases in greenhouse gas emissions, leading to frequent occurrences of extreme weather events such as torrential rains, abnormal heatwaves, and droughts worldwide. These have significant negative impacts on ecosystems and human society[(1)]. Such climate change can trigger social issues that cause enormous global-scale losses, affecting not only the environment but also society as a whole. Therefore, emphasis is being placed on addressing these issues as both short-term and long-term risks[(2)]. To mitigate the impacts of climate change, countries are implementing countermeasures by setting targets for reducing greenhouse gas emissions based on the Paris Agreement[(3)].

*1 Innovation Center, Marketing Headquarters
*2 Innovative Research Excellence, Power Unit & Energy, Honda R&D Co., Ltd.
*3 Corporate Strategy Operations, Honda Motor Co., Ltd.

In the transportation sector, the electrification of automobiles and other forms of mobility is advancing[(1)], and the transition from gasoline vehicles, which emit carbon dioxide during operation, to electric vehicles is being actively promoted by governments worldwide[(4)-(6)]. This shift has led to a rapid increase in the use of lithium-ion batteries for vehicles[(7)], a trend that is expected to continue growing[(8)]. However, alongside the increased number of these batteries in circulation, there is growing concern over counterfeit products. Vehicle lithium-ion batteries have high economic value due to their large capacity and inclusion of rare metals such as cobalt and nickel, making them attractive targets for theft and counterfeiting. The proliferation of counterfeit batteries is a significant safety issue. For example, counterfeit lithium-ion batteries for consumer products such as power tools are widely distributed, and their usage has led to numerous fires[(9)]. To help address this issue, we are developing a non-destructive and non-invasive technology to distinguish between genuine and counterfeit lithium-ion battery packs. In this study, we conducted experiments to determine whether measuring the magnetic flux density during operation can be used to distinguish between genuine and counterfeit battery packs, focusing specifically on those incorporating prismatic and cylindrical cells.

PRIOR RESEARCH

A study conducted by Kong et al. investigated counterfeit lithium-ion batteries(10). According to their findings, counterfeit battery cells include not only newly manufactured illegal products but also those with incorrect model numbers, sizes, or shapes, as well as aged or rejected products that failed to meet quality standards but were disguised externally to resemble genuine products. As a result, highly sophisticated counterfeit batteries that are visually indistinguishable from genuine products are circulating in the market(9).

Genuine battery packs are designed to operate safely through control mechanisms in both the battery cells and the pack itself. In contrast, counterfeit products often have malfunctioning or entirely absent control functions(11), leading to issues such as overvoltage and overcurrent(9), which, in the worst cases, can cause abnormal overheating and fire hazards.

To mitigate these risks, battery manufacturers and manufacturers of battery-powered products have implemented various countermeasures, such as issuing guidelines for identifying counterfeit battery packs and applying hologram seals to warn consumers and indicate authenticity(12). However, as mentioned earlier, highly sophisticated counterfeit products are widespread, limiting the effectiveness of such measures in preventing accidents. Therefore, a detection technology that does not rely on differences in external appearance is needed to identify counterfeit products.

Alternative authentication methods that do not rely on external appearance using QR codes or embedded IC chips(10). However, these methods are not foolproof, as QR codes can be easily copied, and IC chips can be removed from genuine products and installed into counterfeits.

Eto et al.(13) measured the magnetic field around two types of prismatic cells with different electrode forms and confirmed that the spatial distribution of the magnetic field varied depending on the cell type. Based on this, we conducted a more detailed measurement of the magnetic flux density of prismatic cells and verified that each product has a unique magnetic flux density. Furthermore, we found that battery packs incorporating multiple cylindrical cells have individual differences in magnetic flux density due to variations in the manufacturing process. This finding indicates that while the external appearance of a genuine product can be imitated, its magnetic flux density cannot be replicated. Therefore, it is possible to verify whether a battery has been manufactured authentically by measuring magnetic flux density.

CONCEPT FOR DETECTING COUNTERFEIT LITHIUM-ION BATTERIES

Method for Identifying Counterfeits in the Case of Prismatic Cells

The identification of counterfeit prismatic cells relies on the fact that their internal structure varies by model type. In general, current collectors and other internal structural elements of battery cells differ depending on the developer. As a result, when current flows through the battery cell during charging and discharging, differences in current density distribution arise, generating a product-specific magnetic flux density around the battery cell. Therefore, even if a counterfeit product visually resembles a genuine one, differences in internal structure will lead to detectable variations in magnetic flux density, enabling the identification of counterfeit cells.

Method for Identifying Counterfeits in the Case of Cylindrical Cells

In battery packs containing cylindrical cells, individual variations introduced during assembly affect the magnetic flux density of each pack, resulting in different flux patterns even among batteries of the same model.

As shown in Figure 1, components called tabs are used at the positive and negative terminals of cylindrical cells to electrically connect the internal current collection foil to the terminals. During charging and discharging, current concentrates on the tabs, generating locally high magnetic flux density around them and creating a non-uniform flux distribution along the circumference of the cylindrical cell.

Since the position of the tabs is not discernible from the external appearance of the cell, their orientation cannot be deliberately aligned during assembly. Consequently, randomness in tab orientation occurs during battery pack assembly, which influences the magnetic flux density, resulting in a unique flux distribution for each battery pack. By measuring the magnetic flux density at the time of shipment and again during verification, it is possible to confirm whether a battery pack has been manufactured authentically. With this mechanism, even if a counterfeit battery pack is manufactured using the same cylindrical cells and with an external appearance identical to a genuine product, the individual variations in magnetic flux density will enable differentiation between genuine and counterfeit packs.

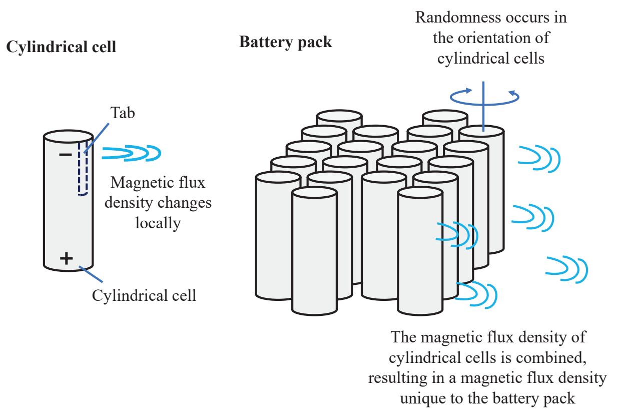

Figure 1 Factors causing individual differences in cylindrical cells

VERIFICATION USING ACTUAL EQUIPMENT

The method described in the previous section was validated by measuring the magnetic flux density generated by a battery during charging and discharging using an actual device. Specifically, the following two points were verified with respect to prismatic and cylindrical cells:

- Prismatic cells with different model numbers each generate distinct magnetic flux densities
- A battery pack incorporating cylindrical cells exhibits a magnetic flux density unique to the individual battery pack

Measurement of Prismatic Cells

a) Experimental method

Figure 2 shows an overview of the measurement setup. Two samples were used, Sample A and Sample B. Both had identical battery performance specifications and external dimensions but had differing model numbers. Measurements were taken along a line 1 mm away from the centerline of the positive electrode side of the cell. A total of 17 points were measured at 5 mm intervals from the top to the bottom of the cell's side surface. A 3 A current was applied to simulate the magnetic flux density generated during charging. To eliminate the influence of geomagnetic fields and other static magnetic fields, the magnetic flux density without applied current was first measured and subtracted from the flux density measured during charging. Below, the measured value refers to the magnetic flux density after subtracting the static magnetic fields.

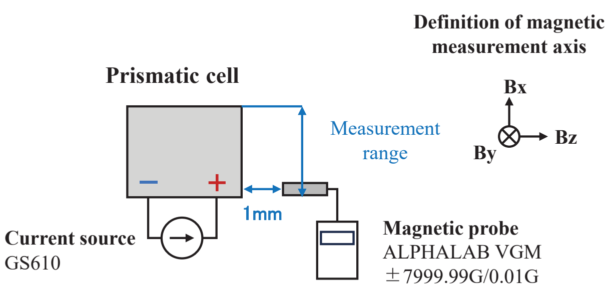

Figure 2 Prismatic cell measurement method

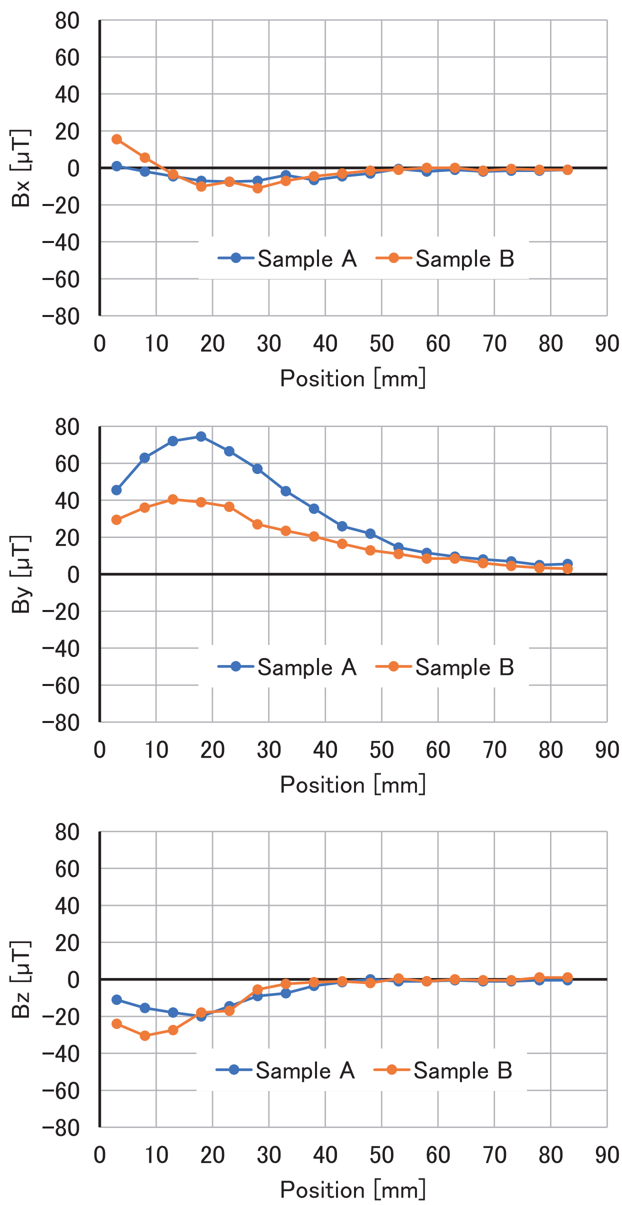

Figure 3 Prismatic cell magnetic flux density measurement results

b) Measurement results

Figure 3 shows the measured magnetic flux density. The vertical axis of each graph represents the measured values (μT), while the horizontal axis represents the measurement positions. The measurement position is defined with the edge on the terminal side of the cell as 0 mm. For both Sample A and Sample B, the peak positions for B_x, B_y, and B_z measured values were observed at approximately 10–20 mm. The absolute values and differences between samples were more pronounced in B_y compared with B_x and B_z. The maximum B_y value was 74.5 μT at 18 mm for Sample A and 40.5 μT at 13 mm for Sample B. Although the absolute values of B_x and B_z were relatively small, differences greater than 1 μT (the sensor's reading margin of error) were observed between samples within the 0–20 mm range.

Measurement of Battery Pack Incorporating Cylindrical Cells

As described in the previous section, the concept of counterfeit detection for cylindrical cells is based on the non-uniform distribution of magnetic flux density in the circumferential direction and the unique magnetic flux density generated in a battery pack due to variations in the angular positioning of cylindrical cells during assembly.

In a preliminary experiment, the magnetic flux density around cylindrical cells was measured to verify the presence of a non-uniform distribution. Subsequently, the magnetic flux density of the battery pack was measured to confirm the existence of individual differences among battery packs.

Measurement of Cylindrical Cell Magnetic Flux Density

a) Experimental method

Figure 4 shows the measurement tool. Eight magnetic sensors were placed 5 mm away from the surface of the cylindrical cell along its axis at 10 mm intervals. The magnetic flux density during charging was measured using these sensors. A triaxial magnetic sensor was used to obtain measured values for three components: the axial component (B_x) along the cylindrical cell's axis, the circumferential component (B_θ), and the radial component (B_r).

Using this measurement tool, the cylindrical cell was measured 24 times at 15-degree intervals from 0 to 360 degrees in the circumferential direction. In the axial direction, a total of 32 measurement points were obtained by scanning the sensor board. As with the prismatic cell measurements, the magnetic flux density without applied current was measured first, and the effect of the static magnetic field was then excluded by calculating the difference from the magnetic flux density when the cylindrical cell was charged with a current of 1.45 A.

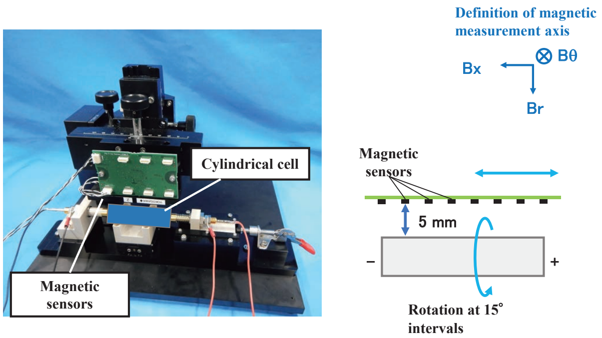

Figure 4 Cylindrical cell measurement tool

b) Measurement results

Figure 5 shows the measurement results of the magnetic flux density during charging. The vertical axis represents the axial coordinate (x) of the cylindrical cell, while the horizontal axis represents the circumferential angle (θ). The x = 0 mm position corresponds to the positive electrode, and the x = 70 mm position corresponds to the negative electrode. Additionally, from the results of Figure 5, Figure 6 shows the magnetic flux density in the circumferential direction at x = 60 mm, near the negative electrode. The most significant variation was observed in the B_θ component of the magnetic flux density, which peaked at 23.6 μT at the 180-degree position. The B_r component also exhibited a non-uniform distribution in the circumferential direction, with a 7.6 μT difference between its maximum and minimum values. In contrast, the B_x component showed minimal variation and remained almost uniform in the circumferential direction.

These results indicate that individual differences in magnetic flux density may arise in a battery pack depending on the orientation of cylindrical cells.

Measurement of Battery Pack Magnetic Flux Density

a) Experimental method

Next, we investigated whether a battery pack incorporating multiple cylindrical cells generates a magnetic flux density unique to the individual unit. Three Honda Mobile Power Pack e: units were measured twice each, and the magnetic flux density was compared between the same unit and different units. As with the magnetic flux density measurements for the cylindrical cell, a dedicated measurement tool and a magnetic sensor array were developed, as shown in Figure 7. The magnetic flux density was measured both with an 8.7 A discharge current applied to the battery pack and with no applied current, and the difference between these values was used as the measured value.

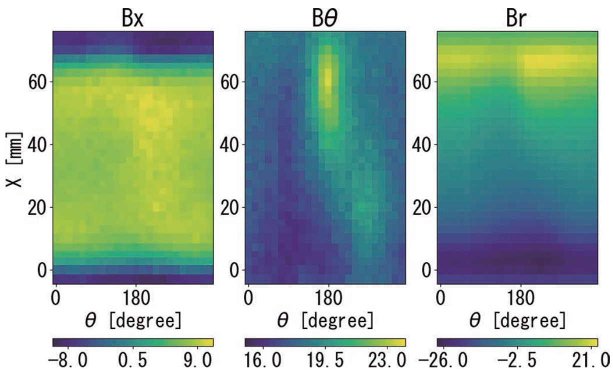

Figure 5 Cylindrical cell magnetic flux density measurement results

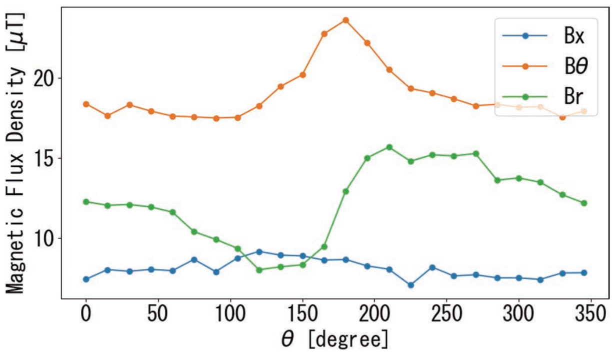

Figure 6 Circumferential magnetic flux density at x = 60 mm position

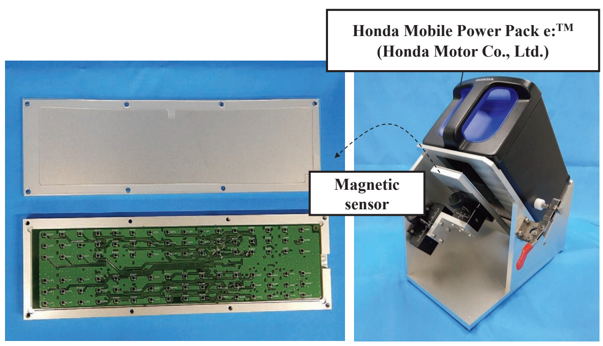

Figure 7 Battery pack measurement tool

b) Measurement results

The measured values and differences between individual units were visualized for the three battery packs, A, B, and C. As a representative example, Figure 8 shows the measured values for Battery Pack A and Battery Pack B. From this figure, no clear differences in magnetic flux density between the battery packs can be observed.

Therefore, two measurements were taken for each battery pack, and the differences between measurements for the same battery pack (Figure 9) and between different battery packs (Figure 10) were visually represented. The differences in measured values for the same battery pack were at the noise level. However, there was a continuous difference in distribution between measured values for Battery Pack B and Battery Pack A, as well as between those for Battery Pack C and Battery Pack A. Table 1 presents the maximum and minimum differences in each distribution shown in Figures 9 and 10, along with the measurement error (±3σ) for B_x, B_y, and B_z, where σ is the unbiased standard deviation calculated from the differences of the same battery pack. For the same battery pack, the maximum difference in measured value was 1.8 μT, whereas for different battery packs, the smallest difference was 5.1 μT (B–A). This difference exceeded the measurement error and was statistically significant.

These results indicate that there are no notable differences in magnetic flux density generated by battery packs at first, as the common signal components present in all battery packs dominate over individual differences. However, by calculating the differences between battery packs and canceling out the common components, it was confirmed that each battery pack has its own unique magnetic flux density.

Table 1 Comparison of maximum-minimum values for each measurement

	B_x (μT)	B_y (μT)	B_z (μT)
A-A	1.6	1.8	1.2
B-B	1.3	1.4	1.0
C-C	1.4	1.5	1.1
B-A	**5.1**	**9.3**	**15.6**
C-A	**7.0**	**10.4**	**13.4**
±3σ	±0.8	±1.1	±0.9

DISCUSSION

Structure of Prismatic Cells and Magnetic Flux Density

Figure 11 illustrates the general structure of a prismatic cell. As shown in the right diagram of Figure 11, the current flows vertically through the electrodes during operation. Accordingly, the B_y component, which is perpendicular to the current flow, tends to be larger than the B_x and B_z components, a trend that was apparent in both samples measured in this experiment. Measuring the B_y component is considered useful for identifying counterfeit prismatic cells, as it captures distinctive characteristics more clearly. Additionally, the peak positions of the B_y and B_z components align with the contact points between the electrode and the winding. In Figure 3, the peak positions of the B_y and B_z components for Sample B are closer to the origin than those for Sample A, and it is confirmed that the actual contact point between the electrode and the winding in Sample B is also positioned closer to the external terminal than in Sample A. There are also differences in the collector structure between the two samples, which may have caused a difference of approximately 20 μT in the peak value of the B_y component. As above, variations in the collector structure and arrangement give rise to differences in the measured values, and each type of cell therefore has a unique magnetic flux density distribution.

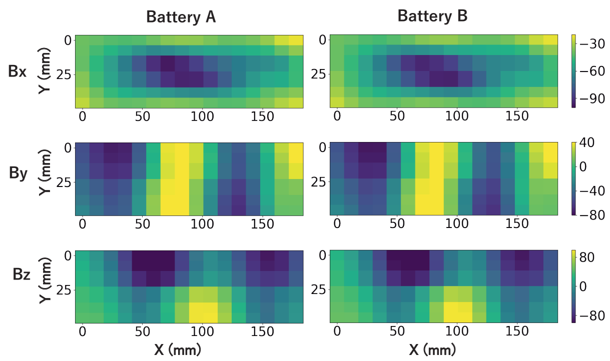

Figure 8 Magnetic flux density of Battery Packs A and B

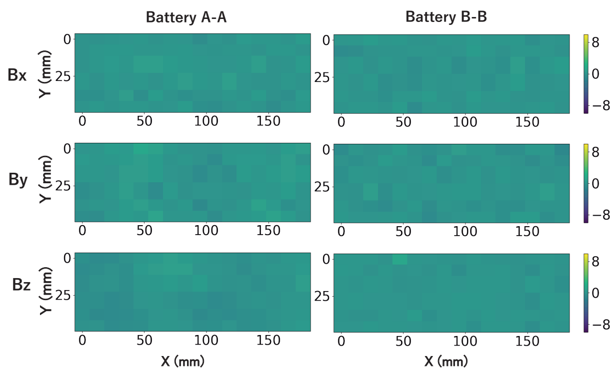

Figure 9 Difference in magnetic flux density in the same unit

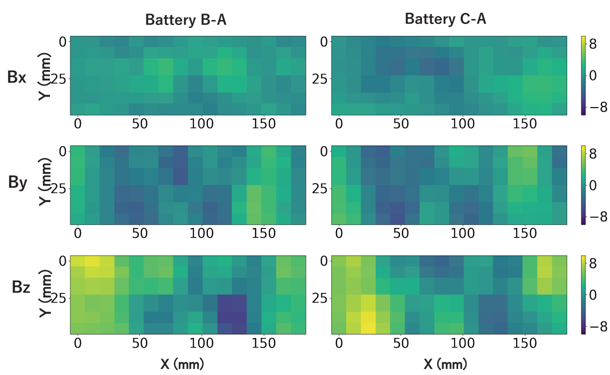

Figure 10 Difference in magnetic flux density between different units

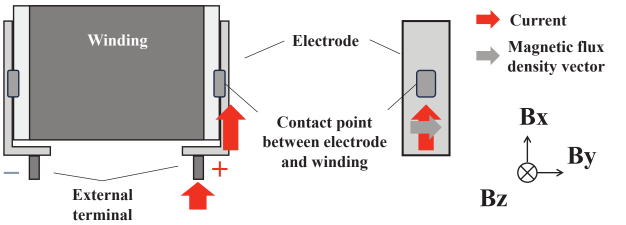

Figure 11 Diagram of entire prismatic cell and electrode

Individual Differences in Cylindrical Cells

Non-uniform magnetic flux density was confirmed to occur in the circumferential direction of cylindrical cells. In particular, a peak in the B_θ component was observed at the 180-degree position, confirming that a negative electrode tab is actually located in this area.

Furthermore, based on Ampère's law, the magnetic flux density appears in the components perpendicular to the current density direction (B_r and B_θ components). In contrast, features caused by the tab were less pronounced in the B_x component, which is parallel to the current direction, resulting in a more uniform distribution (Figure 6).

This trend may also influence the magnetic flux density of the battery pack. As shown in Table 1, the differences between Battery Pack B and Battery Pack A, as well as between Battery Pack C and Battery Pack A, were larger for the B_y and B_z components compared to the B_x component. Additionally, Figure 10 shows that each battery pack exhibits a unique magnetic flux density specific to the individual unit.

Using the identification method described in the earlier section "Concept for detecting counterfeit lithium-ion batteries," these results confirm that the B_r and B_θ components in individual cylindrical cells exhibit a non-uniform distribution of magnetic flux density. Consequently, this non-uniform distribution also leads to individual differences in the magnetic flux density of battery packs incorporating cylindrical cells.

CONCLUSION

In this study, a concept for detecting counterfeit lithium-ion batteries using magnetic flux density was proposed and validated for prismatic and cylindrical cells. The results confirmed that prismatic cells exhibit a unique magnetic flux density depending on the type of cell, and that cylindrical cells have a localized increase in magnetic flux density around the tab area. Furthermore, it was confirmed that the magnetic flux density of battery packs incorporating cylindrical cells (Honda Mobile Power Pack e:) is unique to each unit.

To commercialize a technology for distinguishing between counterfeit and genuine products, a battery authentication method based on magnetic flux density is required. Moving forward, we will work on developing technology for battery authentication using magnetic flux density.

REFERENCES

(1) IPCC, Climate Change 2022: Mitigation of Climate Change. Contribution of Working Group III to the Sixth Assessment Report of the Intergovernmental Panel on Climate Change, Cambridge University Press, 2022, https://www.ipcc.ch/report/ar6/wg3/downloads/report/IPCC_AR6_WGIII_FullReport.pdf, (accessed 2024-07-30)

(2) World Economic Forum, Global Risks Perception Survey 2023-2024, The Global Risks Report 2024 19th Edition, Insight Report, 2024, https://www3.weforum.org/docs/WEF_The_Global_Risks_Report_2024.pdf, (accessed 2024-07-30)

(3) United Nations, United Nations Framework Convention on Climate Change, https://unfccc.int/climate-action, (accessed 2024-09-25)

(4) Ministry of Economy, Trade and Industry, Green Growth Strategy Through Achieving Carbon Neutrality in 2050, https://www.meti.go.jp/policy/energy_environment/global_warming/ggs/pdf/green_koho_r2.pdf, (accessed 2024-07-30), (in Japanese)

(5) Council of the European Union, 'Fit for 55': Council adopts regulation on CO_2 emissions for new cars and vans, March 2023, https://www.consilium.europa.eu/en/press/press-releases/2023/03/28/fit-for-55-council-adopts-regulation-on-co2-emissions-for-new-cars-and-vans/, (accessed 2024-07-30)

(6) The White House, Executive Order on Strengthening American Leadership in Clean Cars and Trucks, August 2021, https://www.whitehouse.gov/briefing-room/presidential-actions/2021/08/05/executive-order-on-strengthening-american-leadership-in-clean-cars-and-trucks/, (accessed 2024-07-30)

(7) International Energy Agency, Global EV Outlook 2024, April 2024, https://iea.blob.core.windows.net/assets/a9e3544b-0b12-4e15-b407-65f5c8ce1b5f/GlobalEVOutlook2024.pdf, (accessed 2024-07-30)

(8) International Renewable Energy Agency, Global Renewables Outlook: Energy transformation 2050, April 2020, https://www.irena.org/-/media/Files/IRENA/Agency/Publication/2020/Apr/IRENA_GRO_Summary_2020.pdf, (accessed 2024-07-30)

(9) National Institute of Technology and Evaluation, Beware of "low price, high risk" non-genuine batteries, 2024, https://www.nite.go.jp/data/000154542.pdf, (accessed 2024-07-30), (in Japanese)

(10) Lingxi Kong, Diganta Das, et al., "The Distribution and Detection Issues of Counterfeit Lithium-Ion Batteries," Energies, Vol. 15, No.10, 2022, 3798

(11) Tapesh Joshi, Saad Azam, et al., "Safety and Quality Issues of Counterfeit Lithium-Ion Cells," ACS Energy Letters, Vol. 8, No. 6,2023, pp. 2831-2839

(12) Francesco Rullani, Karin Beukel, et al., "Anti-counterfeiting strategy unfolded: A closer look to the case of a large multinational manufacturer," Strategic Management Journal, Vol. 42, No. 11, 2021, pp. 2084-2103

(13) Eto, Akimoto, et al., "Study of individual identification method by measuring the magnetic field of battery," Proceedings of Power and Energy Conference, 2022 (in Japanese)